



# A Gradient-Driven Mathematical Model of Antiangiogenesis

A. R. A. ANDERSON AND M. A. J. CHAPLAIN

Department of Mathematics, University of Dundee  
Dundee DD1 4HN, U.K.

C. GARCÍA-REIMBERT AND C. A. VARGAS

FENOMECC & Departamento de Matemáticas y Mecánica  
IIMAS, Universidad Nacional Autónoma de México  
Apdo. 20-726, 01000 Mexico D.F., México

(Received September 1999; revised and accepted April 2000)

**Abstract**—In this paper, we present a mathematical model describing the angiogenic response of endothelial cells to a secondary tumour. It has been observed experimentally that while the primary tumour remains *in situ*, any secondary tumours that may be present elsewhere in the host can go undetected, whereas removal of the primary tumour often leads to the sudden appearance of these hitherto undetected metastases—so-called occult metastases. In this paper, a possible explanation for this suppression of secondary tumours by the primary tumour is given in terms of the presumed migratory response of endothelial cells in the neighbourhood of the secondary tumour. Our model assumes that the endothelial cells respond chemotactically to two opposing chemical gradients: a gradient of tumour angiogenic factor, set up by the secretion of angiogenic cytokines from the secondary tumour; and a gradient of angiostatin, set up in the tissue surrounding any nearby vessels. The angiostatin arrives there through the blood system (circulation), having been originally secreted by the primary tumour. This gradient-driven endothelial cell migration therefore provides a possible explanation of how secondary tumours (occult metastases) can remain undetected in the presence of the primary tumour yet suddenly appear upon surgical removal of the primary tumour. © 2000 Elsevier Science Ltd. All rights reserved.

**Keywords**—Antiangiogenesis, Angiostatin, Endothelial cells, Tumour angiogenic factors, Chemotaxis.

## 1. INTRODUCTION

Solid tumours surmount their dormant avascular state by initiating the formation of new blood vessels from any nearby preexisting vasculature. This development of new blood vessels is known as angiogenesis and is now known to be a crucial step in the metastatic cascade [1]. To start this process, a tumour secretes various chemicals or cytokines, called tumour angiogenic factors (TAFs) [2], into the surrounding tissue or extracellular matrix (ECM). As a consequence, endothelial cells (endothelial cell) lining any neighbouring blood vessels are stimulated into a well-ordered sequence of events beginning with the degradation of their basement membrane.

---

This work was supported by BBSRC Grant 94/MMI09008 and by a FENOMECC (CONACyT G25427-2E) funded visit to UNAM. Dr. Anderson would like to thank all the staff of the mathematics department at UNAM, in particular Cathy and Arturo for their help and hospitality during his visit. Dr. García-Reimbert and Dr. Vargas would like to thank Dr. Chaplain for his hospitality during their stay in Dundee, where this work was initiated.

They then migrate (via chemotaxis) through the ECM towards the tumour [3] and subsequently form small capillary sprouts. These sprouts grow and form loops (anastomoses), and thus, permit a primitive blood circulation. The processes of sprout growth, extension (via endothelial cell migration and proliferation), and loop formation continue until the capillaries eventually reach and penetrate the tumour, thus completing the angiogenic process [3]. At this stage, cells from the primary tumour may escape, migrate through the vasculature into the blood stream and then be deposited at a distant site. These cells from the primary tumour may themselves then continue to grow giving rise to secondary tumours or metastases. The process of cancer cells escaping from the primary tumour, invading the surrounding tissue via the vasculature through intra- and extravasation is known as metastasis [4–6].

A tumour which first initiates angiogenesis, becomes fully vascularised and is detected clinically is named the primary tumour (see Figure 1). It is from this primary tumour, via the process of metastasis, that secondary tumours may arise in other (distant) sites of the host (see Figure 1), as described above. Any metastases which are to grow and survive must undergo precisely the same evolutionary-growth process as the primary tumour, and therefore, at some point in their development will attempt to provoke an angiogenic response in their surrounding tissue to supply the essential nutrients they need to grow and survive. However, Folkman and collaborators [7–9] found that the primary tumour also produces substances that inhibit angiogenesis, so-called antiangiogenic factors. Given that the primary tumour is fully vascularised, these antiangiogenic factors may flood into the blood stream, and therefore, may inhibit the formation of a vasculature around the secondary tumours. Figure 1 gives a schematic diagram of this process. Without their own vasculature, the metastases remain in a dormant state. Further experimental evidence for this has been observed in animal experiments [7,8]. In these experiments, several types of tumour were implanted subcutaneously in mice and allowed to grow. The mice were then examined for the presence of secondary tumours, in particular in the lungs. These results showed little or no evidence for the presence of secondary tumours. However, upon removal of the primary tumour, rapid growth of the hitherto unseen (occult) micrometastases was observed, leading to the growth of many large secondary tumours [8].

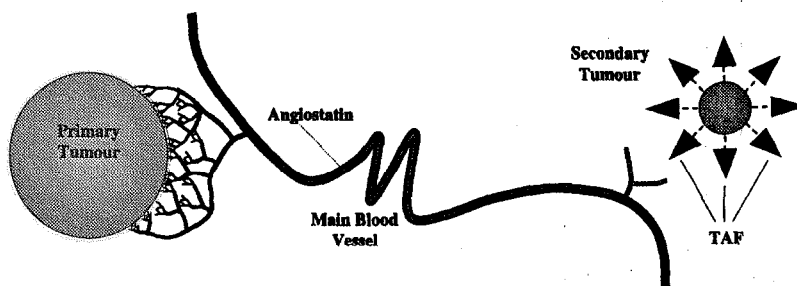


Figure 1. Schematic representation of a fully vascularised primary tumour and its relation to a distant secondary tumour. The cells of the primary tumour secrete angiostatin which enters the blood stream (circulation) via the vascular network. The angiostatin is then transported through the blood stream (circulation) and eventually reaches the parent vessel where an angiogenic response is being elicited by the secondary tumour. Since angiostatin has a relatively long half-life, it is still effective enough to halt the vascularisation of the secondary tumour.

Among the antiangiogenic factors to have been discovered are angiostatin [8] and endostatin [9]. Both of these factors have been shown to inhibit angiogenesis in a dose-dependent manner, i.e., the higher the antiangiogenic factor concentration that is present, the more inhibition of angiogenesis is observed. In particular, angiostatin suppresses both endothelial cell proliferation [8] and migration [10] in a dose-dependent manner. Another important feature of the antiangiogenic effect of angiostatin is its relation with the size of the primary tumour, i.e., the strength of the inhibition is directly proportional to the primary tumour size [9]. In fact, a threshold tumour size is necessary for the inhibitory effect to occur at all [11].

This paper discusses a possible mechanism to explain why a primary tumour can inhibit angiogenesis in a secondary tumour. In particular, we consider a mathematical model for endothelial cell migration in response to gradients of chemical concentration. Using steady-state analysis and numerical simulations, we show that this model can qualitatively reproduce experimentally observed results, such as complete inhibition of angiogenesis, weak vascularisation of the secondary tumour, and successful completion of secondary tumour vascularisation all in relation to the size of the primary tumour.

## 2. THE MATHEMATICAL MODEL

There are many mathematical models which can be found in the literature describing tumour angiogenesis, including deterministic [12–14] and stochastic models [15,16]. Up until now, there have been few which describe explicitly the effects of antiangiogenesis. The models of Orme and Chaplain [17,18] do consider the possible effects of antiproliferative and antichemotactic drugs on endothelial cell activity. However, the effects of these drugs were included in the model only implicitly by changing certain parameters associated with the endothelial cell proliferation and migration. The models also only focussed on the angiogenic response to a primary tumour.

Most of the mathematical models cited above consider partial differential equations describing the motion of endothelial cells, and the equations contain terms representing cell random migration (diffusion), cell biased migration (chemotaxis), cell proliferation, and cell death. Recently, Anderson and Chaplain [12,15] developed a model for angiogenesis that considers endothelial tip-cell migration, i.e., the model considered the motion of the cells located at the tips of the growing sprouts. These models [12,15] have cell migration governed by three factors: diffusion, chemotaxis (in response to TAF gradients), and haptotaxis (in response to gradients of bound macromolecules in the ECM). In a development of these models, we will also consider endothelial cell migration to be governed in part by a chemotactic response to angiostatin.

As already discussed in the Introduction, it is known that angiostatin is a potent antiangiogenic chemical that specifically inhibits endothelial cell proliferation [7,8] and migration [10] in a dose-dependent manner, i.e., the more angiostatin present in the system, the more inhibition there is. We shall therefore assume that the endothelial cells respond chemotactically to angiostatin gradients in a dose-dependent manner.

Since endothelial cell proliferation is inhibited by angiostatin and given that these cells have a long half-life [19] (allowing us to omit birth and death terms) our equation describing cell migration (cf. [12]) is

$$\frac{\partial n}{\partial t} = D_n \frac{\partial^2 n}{\partial x^2} - \frac{\partial}{\partial x} \left( \chi(c)n \frac{\partial c}{\partial x} \right) - \frac{\partial}{\partial x} \left( \alpha(a)n \frac{\partial a}{\partial x} \right), \quad (1)$$

where  $n(x, t)$  is the endothelial cell tip density,  $D_n$  the cell random motility coefficient,  $\chi(c)$  and  $\alpha(a)$  are the TAF chemotactic and angiostatin chemotactic functions, respectively, with  $c(x, t)$  and  $a(x, t)$  representing the TAF and angiostatin concentrations in the one-dimensional domain  $[0, L]$ . We assume that the blood vessel is located at  $x = 0$  and that the secondary tumour is located at  $x = L$ , with host tissue (extracellular matrix) in between.

We assume that the chemotactic function  $\chi(c)$  takes the same form as in [12,15], i.e., we shall assume that endothelial cell receptors become desensitised to high concentrations of TAF, and therefore, take

$$\chi(c) = \chi_0 \frac{k_1}{k_1 + c}, \quad (2)$$

where  $\chi_0$  and  $k_1$  are positive constants representing the maximum chemotactic response and the severity of the desensitisation of endothelial cell to TAF, respectively. To model the dose dependent response of endothelial cells to angiostatin, we assume the following simple linear functional form for  $\alpha(a)$ :

$$\alpha(a) = \alpha_0 a, \quad (3)$$

where  $\alpha_0$  is a positive constant representing the strength of the chemotactic response to angiostatin. Thus, an increase in the angiostatin concentration (as the primary tumour grows larger) will mean an increased chemotactic response from the endothelial cells. Finally, we note that since the mathematical model is considered in one space dimension only, we omit any interactions between the cells and the ECM. These interactions can be modelled more accurately in two and three space dimensions (see [15] for more information).

To model the TAF and angiostatin concentration distributions in the domain we use simple reaction-diffusion models. We assume that the TAF is produced by the secondary tumour (located at  $x = L$ ) and simply diffuses and decays. There will also be some loss of TAF through uptake by the endothelial cells or via sequestering by the extracellular matrix. The angiostatin is produced by the primary tumour, is assumed to be transported through the blood system, and then reaches the parent capillary vessel (located at  $x = 0$ ), where it diffuses into the tissue around the secondary tumour and decays. Once again, there may be some other loss of the chemical as for the TAF. The two equations governing the distribution of the two chemicals concentrations are therefore given by

$$\frac{\partial c}{\partial t} = D_c \frac{\partial^2 c}{\partial x^2} - \lambda_1 c - F(c, n, x), \quad (4)$$

$$\frac{\partial a}{\partial t} = D_a \frac{\partial^2 a}{\partial x^2} - \lambda_2 a - G(a, n, x), \quad (5)$$

where  $F$  and  $G$  are functions modelling the uptake/loss and production of the two chemicals. Although the precise functional forms of  $F$  and  $G$  are unknown, it is expected that any uptake of either chemical can be modelled in a relatively simple manner. For example, previous work [20] has modelled TAF uptake by endothelial cells using Michaelis-Menten kinetics leading to an uptake term of the form  $cn/(1+c)$  while other work [15] has modelled this using an even simpler uptake function  $nc$ . For the purposes of this paper, and in particular, in order to carry out some mathematical analysis, the *precise* functional forms of  $F$  and  $G$  are unimportant (we discuss this in more detail later in this section). As stated previously, the secondary tumour is located at  $x = L$  and we assume that the cancer cells produce and secrete TAF at a rate which enables the TAF concentration here to be kept at a constant value  $c_0$ . The TAF diffuses across the domain and reaches  $x = 0$  but does not penetrate the parent vessel. The TAF is therefore assumed to satisfy the following boundary conditions:  $c = c_0$ ,  $x = L$ ;  $c_x = 0$ ,  $x = 0$ . Similarly, the parent blood vessel is located at  $x = 0$  and we assume that there is sufficient angiostatin reaching here via the bloodstream which enables it to maintain a constant concentration of  $a = A$ . Angiostatin diffuses across the domain, and reaches the secondary tumour at  $x = 1$ . Hence, we assume that the angiostatin concentration satisfies the following boundary conditions:  $a = A$ ,  $x = 0$ ;  $a_x = 0$ ,  $x = L$ . We note that the concentration of angiostatin at the parent vessel  $A$  may vary depending on the size of the primary tumour. Therefore, a high value of  $A$  represents a large primary tumour and a low value of  $A$  represents a small primary tumour.

We now nondimensionalise (1),(4),(5) by rescaling distance with the parent vessel to secondary tumour distance of  $L$ , time with  $\tau = L^2/D_c$  (where  $D_c$  is the TAF diffusion coefficient), endothelial cell density with  $n_0$ , and TAF and angiostatin concentration with  $c_0$  and  $a_0$ , respectively (where  $c_0$  is the TAF concentration at the tumour and  $n_0, a_0$  are appropriate reference variables). Therefore, setting

$$\tilde{c} = \frac{c}{c_0}, \quad \tilde{a} = \frac{a}{a_0}, \quad \tilde{n} = \frac{n}{n_0}, \quad \tilde{t} = \frac{t}{\tau}$$

and dropping the tildes for clarity, we obtain the nondimensional system,

$$\frac{\partial n}{\partial t} = D_1 \frac{\partial^2 n}{\partial x^2} - \frac{\partial}{\partial x} \left( \frac{\chi}{1 + \kappa c} n \frac{\partial c}{\partial x} \right) - \frac{\partial}{\partial x} \left( \alpha a n \frac{\partial a}{\partial x} \right), \quad (6)$$

$$\frac{\partial c}{\partial t} = \frac{\partial^2 c}{\partial x^2} - \gamma_1 c - f(c, n, x), \tag{7}$$

$$\frac{\partial a}{\partial t} = D_2 \frac{\partial^2 a}{\partial x^2} - \gamma_2 a - g(a, n, x), \tag{8}$$

where

$$D_1 = \frac{D_n}{D_c}, \quad D_2 = \frac{D_a}{D_c}, \quad \chi = \frac{\chi_0 c_0}{D_c}, \quad \alpha = \frac{\alpha_0 a_0^2}{D_c},$$

$$\kappa = \frac{c_0}{k_1}, \quad \gamma_1 = \tau \lambda_1, \quad \gamma_2 = \tau \lambda_2.$$

Wherever possible, parameter values have been estimated from available experimental data, and full details can be found in [15]. We assume that the distance from the secondary tumour to the parent vessel ( $L$ ) is between 0.1 and 2 mm [3]. The cell random motility coefficient is taken as  $D_n = 10^{-10} \text{ cm}^2 \text{ s}^{-1}$  (cf. [21]). Stokes *et al.* [16] measured the chemotactic coefficient of migrating endothelial cells in gradients of acidic fibroblast growth factor (aFGF). The maximum chemotactic response was measured in concentrations of aFGF around  $10^{-10} \text{ M}$  giving a chemotactic coefficient of  $2600 \text{ cm}^2 \text{ s}^{-1} \text{ M}^{-1}$ , and therefore, we take  $\chi_0 = 2600 \text{ cm}^2 \text{ s}^{-1} \text{ M}^{-1}$ ,  $c_0 \approx 10^{-10} \text{ M}$ . Estimates for the diffusion coefficient of TAF are in the range  $5 \times 10^{-7}$  to  $5.9 \times 10^{-6} \text{ cm}^2 \text{ s}^{-1}$  [21,22], and for our simulations, we take  $D_c = 2.9 \times 10^{-7} \text{ cm}^2 \text{ s}^{-1}$ . We assume that the diffusion coefficient of angiostatin is of comparable magnitude. It is known from experimental evidence that the decay of TAF is faster than that of angiostatin (experimental observations concerning the half-life for each chemical [1]) and so estimates for the parameters  $\gamma_1, \gamma_2$  may be made using these values. The half-life of angiostatin in the circulation has been estimated at a few hours ( $\sim 4\text{--}6$  hours) and the half-life of VEGF in the circulation (a well-known TAF) has been estimated at a few minutes ( $\sim 3$  minutes) [8]. From these estimates, it is clear that TAF decays more rapidly than angiostatin. In Table 1, we summarise the parameters we have been able to estimate from available experimental data.

Table 1.

Dimensional Parameter	Value	Reference
$D_n$	$10^{-10} \text{ cm}^2 \text{ s}^{-1}$	[21]
$D_c, D_a$	$2.9 \times 10^{-7} \text{ cm}^2 \text{ s}^{-1}$	[21,22]
$\chi_0$	$2600 \text{ cm}^2 \text{ s}^{-1} \text{ M}^{-1}$	[16]
$c_0$	$10^{-10} \text{ M}$	[16]
$L$	2 mm	[3]
$\tau$	1.5 days	
$\lambda_1$	$\sim 3$ minutes	[8]
$\lambda_2$	4–6 hours	[8]

These parameter values now give nondimensional values of  $D_1 = 0.00035$ ,  $\chi = 0.38$ . In the absence of any available data for the angiostatin chemotactic coefficient  $\alpha$ , we assume that this is of the same magnitude as  $\chi$  and so we use a nondimensional value of  $\alpha = 0.38$ . The estimates for  $L$  and  $D_c$  now give the timescale  $\tau = L^2/D_c$  as 1.5 days. Estimating the original decay parameters  $\lambda_1$  and  $\lambda_2$  from the half-life data and then combining these with  $\tau$  yields values for  $\gamma_1$  and  $\gamma_2$  of around 100 and 5, respectively. We summarise the values of the nondimensional parameters used in the subsequent numerical simulations in Table 2.

We impose no-flux boundary conditions on the endothelial cells, that is,

$$\frac{\partial n}{\partial x} = \frac{n}{D_1} \left( \chi(c) \frac{\partial c}{\partial x} + \alpha(a) \frac{\partial a}{\partial x} \right), \quad \text{at } x = 0, 1, \tag{9}$$

Table 2.

Nondimensional Parameter	Value
$D_1$	0.00035
$D_2$	1
$\chi$	0.38
$\alpha$	0.38
$\kappa$	0.1
$\gamma_1$	$\sim 100$
$\gamma_2$	$\sim 5$

and the boundary conditions for the TAF and angiostatin now become

$$c = 1, \quad x = 1; \quad \frac{\partial c}{\partial x} = 0, \quad x = 0 \quad (10)$$

and

$$a = s, \quad x = 0; \quad \frac{\partial a}{\partial x} = 0, \quad x = 1, \quad (11)$$

where  $s = A/a_0$ .

Since the diffusion timescale associated with the two chemicals is much faster than that of the cells, we can assume that the chemicals are in a steady-state with respect to the cells, and therefore, satisfy the following equations:

$$0 = \frac{d^2c}{dx^2} - \gamma_1c - f(c, n, x), \quad (12)$$

satisfying  $c(1) = 1$ ,  $c'(0) = 0$ , and

$$0 = D_2 \frac{d^2a}{dx^2} - \gamma_2a - g(a, n, x), \quad (13)$$

satisfying  $a(0) = s$ ,  $a'(1) = 0$ .

In theory, knowing  $f, g$  explicitly, we may be able to solve (12) and (13) for  $c(x)$  and  $a(x)$ , and then use these solutions to solve only one equation, namely (6). However, even if functions  $f$  and  $g$  are known exactly, it may not be possible to do this. In the simple case where we assume no other loss or uptake of the chemicals apart from simple decay, one can easily show that the closed-form solutions to

$$0 = \frac{d^2c}{dx^2} - \gamma_1c, \quad c(1) = 1, \quad c'(0) = 0, \quad (14)$$

$$0 = D_2 \frac{d^2a}{dx^2} - \gamma_2a, \quad a(0) = s, \quad a'(1) = 0 \quad (15)$$

are given by

$$c(x) = \frac{\cosh(\sqrt{\gamma_1}x)}{\cosh\sqrt{\gamma_1}} \quad (16)$$

and

$$a(x) = s \frac{\cosh\left[\sqrt{(\gamma_2/D_2)}(1-x)\right]}{\cosh\sqrt{(\gamma_2/D_2)}}. \quad (17)$$

Finally, we close the system for the endothelial cells by imposing appropriate initial conditions. With the secondary tumour located at  $x = 1$  and the parent vessel (source of the angiostatin via the primary tumour) of the endothelial cells located at  $x = 0$ , we take

$$n(x, 0) = e^{-x^2/(0.005)}, \quad 0 \leq x \leq 1, \quad (18)$$

as the initial distribution of endothelial cells. This simple form is chosen to model the fact that endothelial cells in the initial capillary sprouts are located close to the parent vessel.

### 3. ANALYTICAL AND NUMERICAL SOLUTIONS OF THE MODEL

In this section, we analyse our model both analytically and numerically. Since we are interested in whether or not the tumour becomes vascularised, i.e., whether or not endothelial cells at the tips of the capillaries connect with the tumour after some period of time, it is appropriate to examine the steady-state behaviour of our model.

Therefore, we now examine the steady-state solutions of (6) with boundary conditions (9). Setting  $\frac{\partial n}{\partial t} = 0$  and integrating (6) with respect to  $x$  gives

$$E_1 = D \frac{\partial n}{\partial x} - \chi(c)n \frac{\partial c}{\partial x} - \alpha(a)n \frac{\partial a}{\partial x}.$$

Applying the boundary conditions (9) gives  $E_1 = 0$ , and hence,

$$\frac{\partial n}{\partial x} = \frac{n}{D} \left( \frac{\chi_0}{1 + \kappa c} \frac{\partial c}{\partial x} + \alpha_0 a \frac{\partial a}{\partial x} \right). \tag{19}$$

Integrating (19) then yields the steady-state solution

$$n(x) = E_2 \exp \left[ \frac{\chi_0}{D\kappa} \ln(1 + \kappa c(x)) + \frac{\alpha_0}{2D} a(x)^2 \right], \tag{20}$$

where  $E_2$  is a constant of integration chosen to ensure conservation of endothelial cell density. Since both terms within the exponential function of (20) are always positive, the steady-state solution will depend upon which of these terms is larger, i.e., if the primary tumour is larger then more angiostatin is produced and the term  $(\alpha_0/2D)[a(x)]^2$  will dominate. Given the functional form of  $a(x)$  (cf. (22)), all the endothelial cells will be held (via chemotaxis) close to the parent vessel at  $x = 0$ . The reverse is true if the primary tumour is small (or the secondary is larger). In this case, the term  $(\chi_0/D\kappa) \ln(1 + \kappa c(x))$  will dominate the solution and so the endothelial cells will migrate (via chemotaxis) to the tumour at  $x = 1$ , thus, completing vascularisation. Clearly, these results are dependent upon the relative sizes of  $\chi_0$ ,  $\kappa$ , and  $\alpha_0$ .

In order to investigate the model further, both analytically and numerically, we must consider explicit functional forms for  $a(x)$  and  $c(x)$ . However, since the precise functional forms of  $f$  and  $g$  are unknown, we make the simplifying assumption that the steady-state profiles of TAF and angiostatin are qualitatively similar to those of (16) and (17), i.e., the steady-state TAF concentration profile is a monotonic increasing function on  $x \in [0, 1]$  and the steady-state angiostatin concentration profile is a monotonic decreasing function on  $x \in [0, 1]$ . We therefore take

$$c(x) = e^{-(1-x)^2/\epsilon_2}, \quad 0 \leq x \leq 1, \tag{21}$$

and

$$a(x) = se^{-x^2/\epsilon_1}, \quad 0 \leq x \leq 1, \tag{22}$$

where  $\epsilon_2$  and  $\epsilon_1$  are both small positive constants with  $\epsilon_2 < \epsilon_1$ . This models the faster decay of TAF compared with angiostatin. The parameter  $s$  is a positive constant directly proportional to the size of the primary tumour. As discussed in the introduction, angiostatin is produced by the primary tumour and then flows through the circulation to a vessel close to the secondary tumour. It is known that the inhibitory effect of the primary tumour upon a secondary tumour is directly proportional to the size of the primary [8], thus, the amount of angiostatin produced depends on the size of the primary tumour. Plots of (18), (21), (22) are given in Figure 2, for  $\epsilon_1 = 0.6$ ,  $\epsilon_2 = 0.2$ , and  $s = 1.0, 1.404, 1.6$ . Clearly as  $s$  increases, the concentration of angiostatin increases through the whole domain.

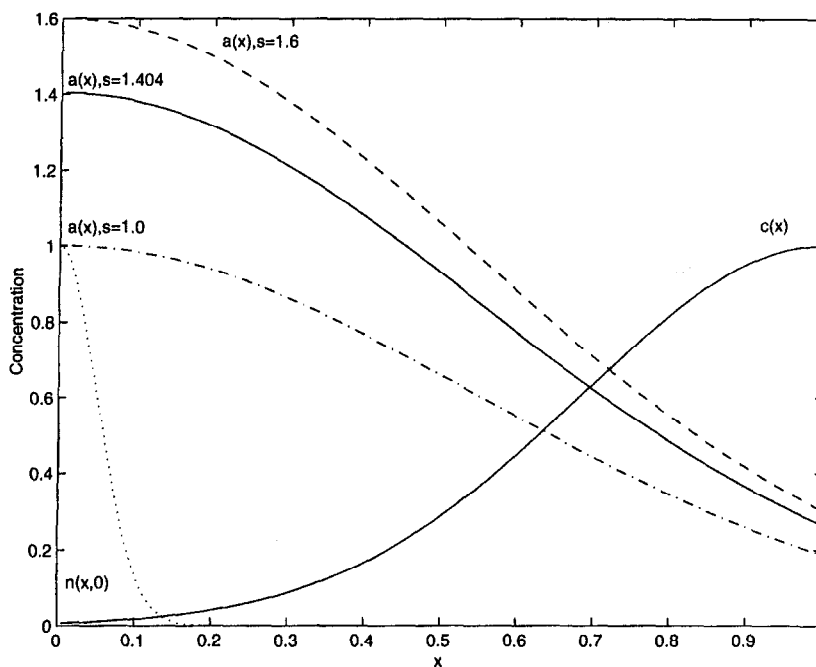


Figure 2. Initial endothelial cell density profile (from equation (16)); initial concentration profiles of angiostatin (from equation (17)) for  $s = 1.0, 1.404, 1.6$ ; initial TAF concentration profile (from equation (18)). Parameter values are  $\epsilon_1 = 0.6$  and  $\epsilon_2 = 0.2$ .

To examine the effect of primary tumour size upon the angiogenic response to a secondary tumour, we considered the solution profiles of (20) using the TAF and angiostatin profiles (21) and (22) for three different sizes of primary tumour (under the assumption that tumour size is directly proportional to the amount of angiostatin produced). We considered a large tumour ( $s = 1.6$ ), a medium-sized tumour ( $s = 1.404$ ), and small tumour ( $s = 1.0$ ) (see Figure 2 for how the concentration profiles of angiostatin change with these different parameters).

Figure 3 shows the steady-state solutions obtained from (20) for the three values of  $s$ . As expected for a large primary tumour ( $s = 1.6$ ), the endothelial cells remain close to the parent vessel and vascularisation of the tumour fails. For a small primary tumour ( $s = 1.0$ ), the endothelial cells reach the secondary tumour and vascularisation is completed. More interestingly, for a medium-sized tumour ( $s = 1.404$ ), some endothelial cells remain close to the parent vessel and some endothelial cells reach the secondary tumour. This may represent a weak vascularisation of the secondary tumour. Chen *et al.* show that such a weak vascularisation can occur, with only a few capillary sprouts connecting with the secondary tumour [23].

The values of  $s$  were chosen to illustrate the range of behaviour our model can produce. Other values of  $s$  work equally well, e.g., from our investigations, we found that  $s \geq 1.6$  gives no vascularisation,  $s \leq 1.0$  gives complete vascularisation and  $1.0 < s < 1.6$  produces weak vascularisation.

To verify the steady-state results we solved equation (6) numerically using the NAG routine D03PCF. Taking the same parameter values used for Figure 3 and the boundary and initial conditions given by (9),(18)–(21), we produced Figure 4. The numerical steady states for  $s = 1.0$ ,  $s = 1.404$ , and  $s = 1.6$  match the analytical solutions closely, thus, verifying the analytical results.

In addition to the above steady-state analysis and numerical simulations, further investigations were carried out which we report here. We examined the solution for  $n$  from (20) using the steady-state profiles for  $c(x)$  and  $a(x)$  given by (16) and (17) and found qualitatively similar results to those of Figure 3. Finally, we also carried out numerical simulations on the full time-dependent equations (6)–(8) with explicit uptake functions  $f = \beta_1 nc$  and  $g = \beta_2 na$ . Once again, we found

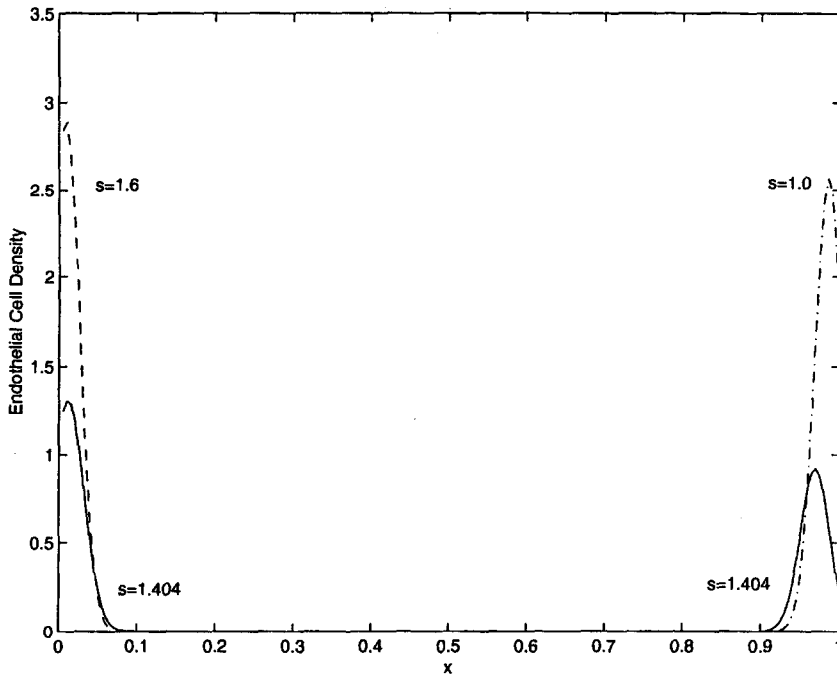


Figure 3. Steady-state solutions of (20) showing the final profile of the endothelial cell density for three different values of the parameter  $s = 1, 1.404, 1.6$ . Other parameter values:  $\epsilon_1 = 0.6, \epsilon_2 = 0.2, D = 0.00035, \kappa = 0.1, \chi_0 = \alpha_0 = 0.38$ .

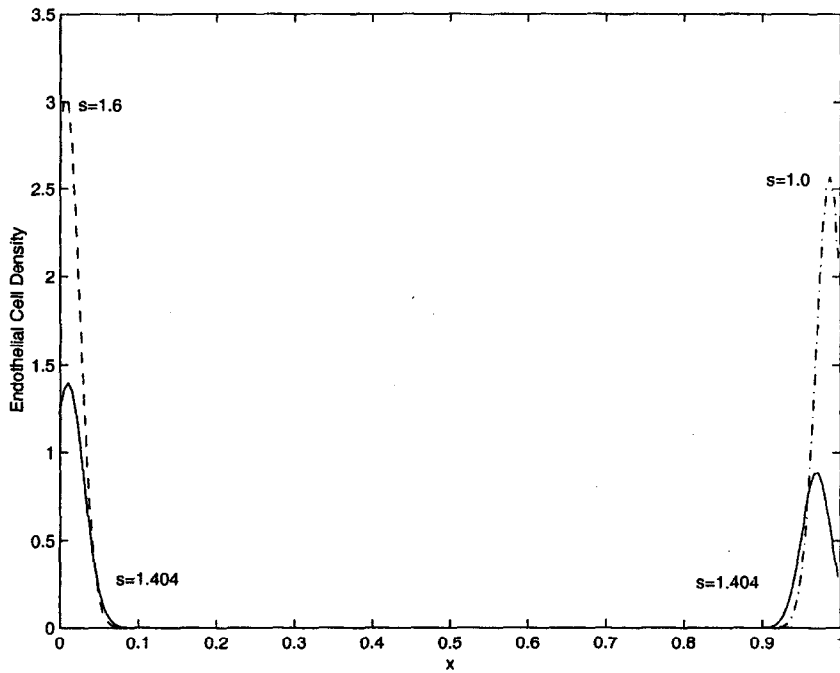


Figure 4. Steady-state solutions obtained from numerical simulation of (6) obtained at a time of  $t = 1000$ . Parameters values as per Figure 3, for  $s = 1, 1.404, 1.6$ .

that the long time results for the endothelial cell density profiles were in qualitative agreement with those shown in Figures 3 and 4.

As shown experimentally, removal of the primary tumour leads to vascularisation of secondaries and subsequent growth [8]. In order to model this behaviour, we mathematically remove the primary tumour. In this case, angiostatin is no longer in steady state, and hence, we consider a

time-dependent equation for angiostatin, i.e.,

$$\frac{\partial a}{\partial t} = D_2 \frac{\partial^2 a}{\partial x^2} - \gamma_2 a, \quad (23)$$

satisfying  $\frac{\partial a}{\partial x} = 0$  at  $x = 0, 1$ . The boundary condition at  $x = 0$  now reflects the fact that there is no source of angiostatin, i.e., there is no primary tumour since this has been removed. We now solve equations (6), (7), and (21) numerically to obtain Figure 5 (with  $f = 0$ ). This figure shows the results of removing the primary tumour, with the same initial data and other parameters as in Figure 4, and the parameter  $\gamma_2 = 5$ . The profile of the endothelial cell density is given at times  $t = 0, 1, 4, 10$ . As can be seen from the results, as time increases (and the angiostatin decays), the endothelial cell population gradually moves across the domain via chemotaxis until at  $t = 10$  the whole population of the cells has connected with the tumour and completed vascularisation. Subsequently, the vascularised secondary tumour will grow rapidly as observed experimentally.

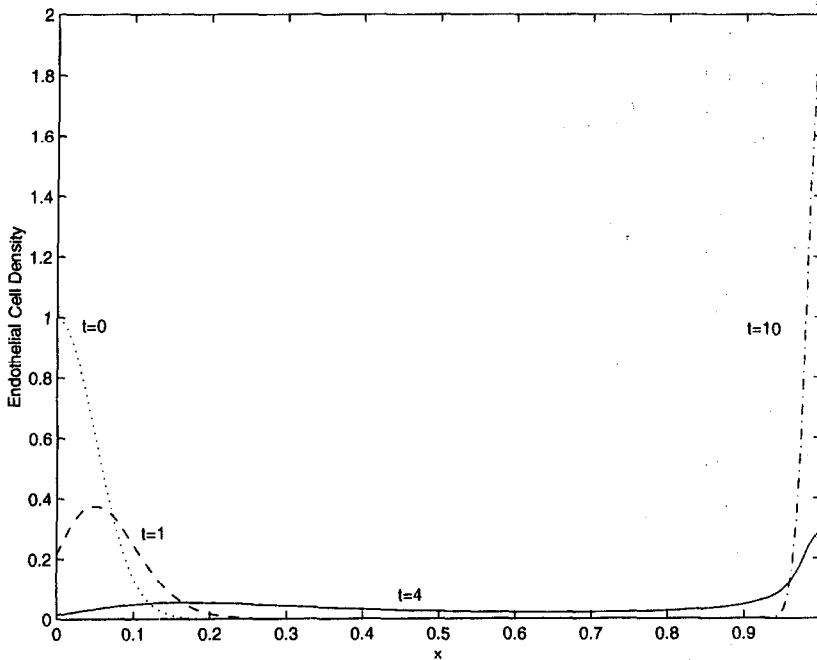


Figure 5. Profiles of the endothelial cell density at times  $t = 0, 1, 4, 10$  in the case where the primary tumour is removed. In this case, the angiostatin decays, the gradient of angiostatin therefore tends to zero thus enabling the endothelial cells to migrate to the tumour and complete vascularisation.

These simulation results are in qualitative agreement with the results and observations of Retsky *et al.* [24] and Holmberg and Baum [25] concerning the effect of surgery on the growth of secondary tumours. These papers hypothesise that while the primary tumour remains, any secondary tumours (micrometastases) are in a state of “dynamic equilibrium” and are either poorly vascularized or completely avascular. Upon removal of the primary tumour, this dynamic equilibrium is perturbed leading to the vascularization and subsequent growth of some of the secondary tumours. In our model, a value of  $s > 1$  will result in either weak or no vascularization. As we have shown above in Figure 5, removal of the primary leads to a loss of the angiostatin (perturbing the equilibrium) and subsequent vascularization.

#### 4. CONCLUSIONS AND DISCUSSION

We have presented a simple mathematical model which describes the control of secondary tumour growth via the primary tumour in a novel manner. The model extends and develops

previous models of antiangiogenesis [17,18] via the inclusion of an explicit equation for an antiangiogenic chemical, such as angiostatin, by building on the work of Anderson and Chaplain [12] concerning tumour vascularization. Specifically, our model assumes that an antiangiogenic chemical (e.g., angiostatin) is produced by the primary tumour and is transported via the circulation to any sites of secondary tumour growth [8,9]. At these locations, we assume that any secondary tumours are already secreting TAF and eliciting an angiogenic response from neighbouring vessels and that endothelial cells there have caused some disruption to these vessels [19,26]. The antiangiogenic chemical then enters the tissue through any disrupted parent vessels and diffuses into the host tissue surrounding the secondary tumour, setting up a concentration gradient. The main assumption of the model is that the endothelial cells also respond chemotactically to the gradient of angiostatin and so must now respond to two opposing gradients, i.e., the gradients of the antiangiogenic chemical and also the TAF, and their subsequent motion will be governed by the relative strength of each. Our results show that by varying the size of the primary tumour (via the level of angiostatin at the parent vessel), we can qualitatively obtain a range of behaviour that is observed experimentally, i.e., no vascularisation, weak vascularisation, and complete vascularisation of the secondary tumour.

These results are based on the assumption that the secondary tumour is close enough to the parent vessel for initiation of angiogenesis to occur. This means that, in the absence of antiangiogenic factors, vascularization of the secondary tumour will always occur. *In vivo*, of course, it is expected that there will be some secondary tumours which remain avascular (i.e., are *not* vascularised) even after removal of the primary tumour. Our model could account for this if we located the secondary tumour further from the parent vessel or if the decay rate of TAF was increased. By extending the model to two or three dimensions, we could include explicit interactions between the EC and the ECM [15]. However, this would not qualitatively change the above results although the rate of capillary growth may be slowed, in line with the results of Anderson and Chaplain [15]. We would also be able to obtain a more detailed description of the resulting capillary network with a discrete form of the model, including the number of branches and anastomoses [12,15]. Such a discrete model allows for the tracking of individual EC and could therefore be used to explicitly investigate the effect of antiangiogenic drugs upon EC proliferation (see [15] for a more detailed discussion on the discrete modelling of angiogenesis).

Finally, when developing our model, we assumed that endothelial cells respond chemotactically to angiogenic inhibitors (e.g., angiostatin and endostatin). This hypothesis could be proved experimentally but, to our knowledge, such experiments have not yet been conducted.

## REFERENCES

1. J. Folkman, Angiogenesis in cancer, vascular, rheumatoid and other disease, *Nature Med.* **1**, 27–31 (1995).
2. J. Folkman and M. Klagsburn, Angiogenic factors, *Science* **235**, 442–447 (1987).
3. V.R. Muthukkaruppan, L. Kubai and R. Auerbach, Tumour-induced neovascularization in the mouse eye, *J. Natl. Cancer Inst.* **69**, 699–705 (1982).
4. A.F. Chambers and L.M. Matrisian, Changing views of the role of matrix metalloproteinases in metastasis, *J. Natl. Cancer Inst.* **89**, 1260–1270 (1997).
5. J.A. Lawrence and P.S. Steeg, Mechanisms of tumour invasion and metastasis, *World J. Urol.* **14**, 124–130 (1996).
6. W.G. Stetler-Stevenson, S. Aznavoorian and L.A. Liotta, Tumor cell interactions with the extracellular matrix during invasion and metastasis, *Ann. Rev. Cell Biol.* **9**, 541–573 (1993).
7. J. Folkman, Angiogenesis in cancer, vascular, rheumatoid and other disease, *Nature Med.* **1**, 27–31 (1995).
8. M.S. O'Reilly, L. Holmgren, Y. Shing, C. Chen, R.A. Rosenthal, M. Moses, W.S. Lane, Y. Cao, E.H. Sage and J. Folkman, Angiostatin: A novel angiogenesis inhibitor that mediates the suppression of metastases by Lewis lung carcinoma, *Cell* **79**, 315–328 (1994).
9. M.S. O'Reilly, T. Boehm, Y. Shing, N. Fukami, G. Vasios, W.S. Lane, E. Flynn, J.R. Birkhead, B.R. Olsen and J. Folkman, Endostatin: An endogenous inhibitor of angiogenesis and tumour growth, *Cell* **88**, 277–285 (1997).
10. W.-R. Ji, F.J. Castellino, Y. Chang, M.E. Deford, H. Gray, X. Villarreal, M.E. Kondri, D.N. Marti, M. Llinas, J. Schaller, R.A. Kramer and P.A. Trail, Characterization of kringle domains of angiostatin as antagonists of endothelial cell migration, an important process in angiogenesis, *FASEB* **12**, 1731–1738 (1998).

11. J.C. Himmele, B. Rabenhorst and D. Werner, Inhibition of Lewis lung tumor growth and metastasis by Ehrlich ascites tumor growing in the same host, *J. Cancer Res. Clin. Oncol.* **111**, 160–165 (1986).
12. A.R.A. Anderson and M.A.J. Chaplain, A mathematical model for capillary network formation in the absence of endothelial cell proliferation, *Appl. Math. Lett.* **11** (3), 109–114 (1998).
13. M.A.J. Chaplain, Avascular growth, angiogenesis and vascular growth in solid tumours: The mathematical modelling of the stages of tumour development, *Mathl. Comput. Modelling* **23** (6), 47–88 (1996).
14. D. Balding and D.L.S. McElwain, A mathematical model of tumour-induced capillary growth, *J. Theor. Biol.* **114**, 53–73 (1985).
15. A.R.A. Anderson and M.A.J. Chaplain, Continuous and discrete mathematical models of tumour-induced angiogenesis, *Bull. Math. Biol.* **60**, 857–899 (1998).
16. C.L. Stokes and D.A. Lauffenburger, Analysis of the roles of microvessel endothelial cell random motility and chemotaxis in angiogenesis, *J. Theor. Biol.* **152**, 377–403 (1991).
17. M.E. Orme and M.A.J. Chaplain, Two-dimensional models of tumour angiogenesis and anti-angiogenesis strategies, *IMA J. Math. Appl. Med. Biol.* **14**, 189–205 (1997).
18. M.A.J. Chaplain and M.E. Orme, Mathematical modeling of tumor-induced angiogenesis, In *Vascular Morphogenesis: In Vivo, In Vitro, In Mente*, (Edited by C. Little, E.H. Sage and V. Mironov), Chapter 3.4, pp. 205–240, Birkhauser, Boston, MA, (1998).
19. N. Paweletz and M. Knierim, Tumour-related angiogenesis, *Crit. Rev. Oncol. Hematol.* **9**, 197–242 (1989).
20. M.A.J. Chaplain and A.M. Stuart, A model mechanism for the chemotactic response of tumour cells to tumour angiogenesis factor, *IMA J. Math. Appl. Med. Biol.* **10**, 149–168 (1993).
21. D. Bray, *Cell Movements*, Garland Publishing, New York, (1992).
22. J.A. Sherratt and J.D. Murray, Models of epidermal wound healing, *Proc. R. Soc. Lond.* **B241**, 29–36 (1990).
23. C. Chen, S. Parangi, M.J. Tolentino and J. Folkman, A strategy to discover circulating angiogenesis inhibitors generated by human tumours, *Cancer Res.* **55**, 4230–4233 (1995).
24. M.W. Restky, R. Demicheli, D.E. Swartzendruber, P.D. Bame, R.H. Wardwell, G. Bonadonna, J.F. Speer and P. Valagussa, Computer simulation of a breast cancer metastasis model, *Breast Cancer Res. Treat.* **45**, 193–202 (1997).
25. L. Holmberg and M. Baum, Work on your theories!, *Nat. Med.* **2**, 844–846 (1996).
26. S. Paku and N. Paweletz, First steps of tumor-related angiogenesis, *Lab. Invest.* **65**, 334–346 (1991).
27. M.M. Sholley, G.P. Ferguson, H.R. Seibel, J.L. Montour and J.D. Wilson, Mechanisms of neovascularization. Vascular sprouting can occur without proliferation of endothelial cells, *Lab. Invest.* **51**, 624–634 (1984).